Dual wideband printed dipole antenna with integrated balun

P. Lindberg, E. Öjefors, Z. Barna, A. Thornell-Pers and A. Rydberg

Abstract: A printed dipole antenna with integrated balun is presented. The radiating structure is a two-element dipole with resonances at 900 and 1700 MHz, with the balun providing one extra resonance at each band. By co-designing the radiating element with a Marchand balun modified for dual-band operation, an antenna covering the cellular bands 824–960 and 1710–2170 MHz has been achieved. Measurements on a fabricated antenna on low-cost FR-4 substrate show antenna efficiencies of >80 and >70% in the lower and upper band respectively. Despite the use of a dual-element radiator, the radiation pattern that is close to omni-directional H-plane is obtained.

1 Introduction

Wireless terminals today are typically required to support several communication systems and bands, such as GSM 850 and 900 MHz, PCS/DCS 1800 and 1900 MHz, UMTS 2.1 GHz, WLAN 2.4 and 5 GHz and so on. Usually, a single multi-band RF transceiver module covers all related systems (e.g. cellular) supported by the terminal to reduce component count, prize, volume and power consumption. To be compatible with the transceiver and from size constraints, a single antenna using a single (typically unbalanced) feed point that covers all bands supported by the transceiver is needed. The main challenge in terminal antenna design is therefore, since directivity is normally not an issue, to fulfil the bandwidth requirements of the various systems with sufficient antenna efficiency. If possible, the antenna should also have omni-directional radiation properties at all bands. For reasons of ease and cost of production, low profile and low weight, antennas printed on PCBs are generally preferred.

For cellular applications, the GSM and UMTS frequency bands partially overlap, meaning that the antenna does not need to provide five separate resonances but rather two wide-bands, 824–960 MHz (>15% relative bandwidth) and 1710–2170 MHz (>23% relative bandwidth). WLAN applications at 2.4 GHz (IEEE 802.11b and IEEE 802.11g) and 5 GHz (IEEE 802.11a) have similar requirements and frequency spacing, but are less demanding in this respect with <3 and 12.3% relative bandwidths, respectively.

Several printed antennas for omni-directional dual-band cellular or WLAN applications have been reported in the literature. A dual dipole structure, with a short element providing resonance at the upper frequency band in parallel with a long element resonating at a lower frequency band, was presented for GSM900/1800/1900 or WLAN 2.4/5.2 GHz applications in [1]. Insufficient bandwidth to cover all cellular bands was however obtained, and no dual-band/wideband balun was provided. A similar antenna element for WLAN 2.4/5.2 GHz was presented in [2], together with a microstrip to balanced Lecher line-type transition [3] acting as a balun. Measured bandwidths at the lower and upper frequency bands were 9.3 and 5.1%, respectively, which is insufficient for the targeted application in this paper. Other dual-band dipoles without baluns, and hence unsuitable for connection to a single-ended transceiver, are presented in [4–8]. Additionally, the reported performance of the antennas in these papers is somewhat unreliable, as the coaxial cable used during measurements was not decoupled by a balun and hence radiating currents on the outside of the coaxial shield contributed to the measured parameters. An antenna was presented in [9], using two series-fed dipole pairs separated by 40 mm to provide dual-band functionality at 900 and 1800 MHz. A 45 mm long microstrip-to-parallel-stripline-tapered transition was used as a balun and to transform the 57 Ω antenna impedance into 50 Ω, that is, the balun was not designed to compensate for the reactive part of the antenna impedance. No measured bandwidth for an antenna without reflector was reported, but from the calculated input impedance presented, it is estimated that it is not sufficient to cover all cellular bands. Kim *et al.* [10] proposed the use of a spiralled dipole structure as a compact dual-band WLAN 2.4/5.8 GHz antenna, including a tapered microstrip line balun. The bandwidth was however too narrow (17 and 10% at 2.4 and 5.8 GHz, respectively) to cover all cellular bands, and the radiation pattern exhibited two extra deep nulls compared with a standard dipole. A dual dipole antenna with a wideband transition from unbalanced microstrip line to balanced CPS was presented in [11]. Unfortunately, very few design details about the transition were given; the antennas were $\simeq\lambda$ long at each band (and hence twice as long as standard dipoles) and the reported bandwidth at the upper frequency band was too narrow (18.75 and 7.7% at 2.4 and 5.2 GHz, respectively) for the application intended in

doi:10.1049/iet-map:20050286

Paper first received 22nd November 2005 and in revised form 8th January 2007

P. Lindberg, E. Öjefors and A. Rydberg are with the Department of Engineering Sciences, Signals and Systems Group, Uppsala University, Box 528, SE 751 02 Uppsala, Sweden

A. Thornell-Pers is with Laird Technologies, Box 500, SE 184 25 Åkersberga, Sweden

Z. Barna is with the BetaWave Bt., Vizisport ut 23/a., Budapest, 1203, Hungary

P. Lindberg is also with Laird Technologies, Box 500, SE 184 25 Åkersberga, Sweden

E-mail: peter.lindberg@signal.uu.se

this paper. Wideband dipoles using Marchand baluns [12] were reported in [13–15] and modified for dual-band 900/1800 MHz operation in [16] by using a T-shaped radiator and changing the lengths of the stubs in the balun. Measured bandwidths were 15.6% at 900 MHz and 12% at 1800 MHz, which is not sufficient for the targeted application here.

In this paper, we present a printed dual-band antenna in which the radiating element and integrated balun have been co-optimised to provide two resonances in each band to increase the impedance bandwidth, a technique that has so far only been used for single-band dipole antennas [13–15]. The concept has been demonstrated with an implementation on low-cost FR-4 substrate, covering the 824–960 and 1710–2170 MHz frequency bands. By modifying the topology of the classical Marchand balun for dual-band functionality and adjusting the radiating element for a suitable frequency response, a dual wideband impedance match has been obtained. Design details of the radiating element and balun are provided together with measured and simulated results. An equivalent circuit model is also provided to facilitate rapid optimisation of the balun structure, using linear circuit simulation tools. To the authors' knowledge, this is the first printed dual-band dipole antenna, including a dual-band balun structure, presented that provides good performance in all four GSM bands as well as in UMTS 2.1 GHz.

Typical applications for the proposed antenna are terminal-related products such as M2M communication, telematic units, repeaters, base stations, internal or external car-mounted antennas and WLAN-cellular wireless access points. The concept is easily extended to WLAN 2.4 and 5 GHz applications, for example, for use in laptops or routers.

2 Antenna design

2.1 Radiating element

A dual dipole structure is used as a radiating element (Fig. 1), which provides resonances at ≃900 and 1700 MHz (Fig. 2) (simulated data from EM software IE3D [17], the frequency limits of interest are marked with vertical lines). The long dipole provides 900 MHz resonance, whereas the short dipole provides 1700 MHz resonance. The long dipole is nearly unaffected by the presence of the short dipole, the main effect being a minor increase of shunt capacitance at the feed terminals, as can be seen in Fig. 3. In terms of impedance, the short dipole is also almost unaffected by the long dipole because at about 1800 MHz, the long dipole presents a second high impedance (anti-) resonance. Because of this effect, stemming from the approximate ×2 frequency spacing of the two bands, it is possible to tune the two resonances individually without significant mutual coupling. In the lower frequency band, the radiation characteristic is nearly identical to a single dipole element. However, the high-frequency radiation properties are slightly altered because of the long dipole acting as a reflector for the short dipole, thus increasing the gain. All dipole arms have been chamfered close to the feed gap to minimise the shunt capacitance, which is especially significant at the upper frequency band. Instead of designing both dipoles for minimum return loss in each respective band, the shorter dipole was made somewhat longer to give the impedance loci shown in Fig. 3. This provides a more suitable starting point for the impedance transformations introduced by the balun described in the following section. Finally, it should be noted that although a two-element dipole antenna has a reasonably

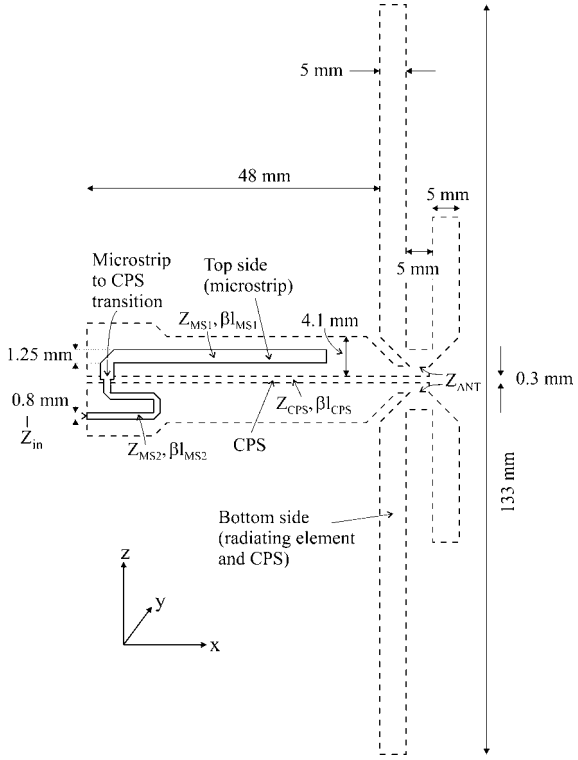

Fig. 1 *Schematic drawing of radiator and balun structure*

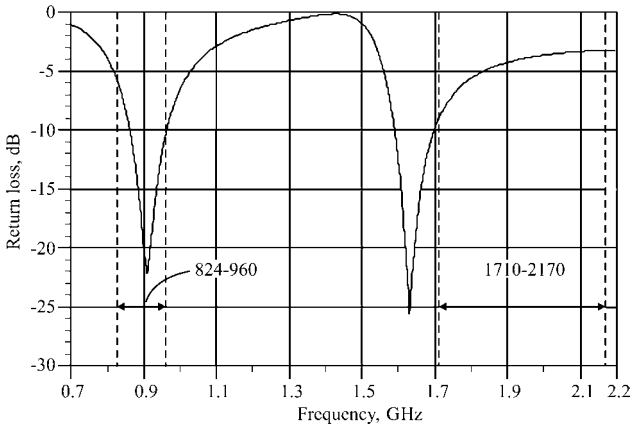

Fig. 2 *Simulated return loss of radiating element without balun/matching network*

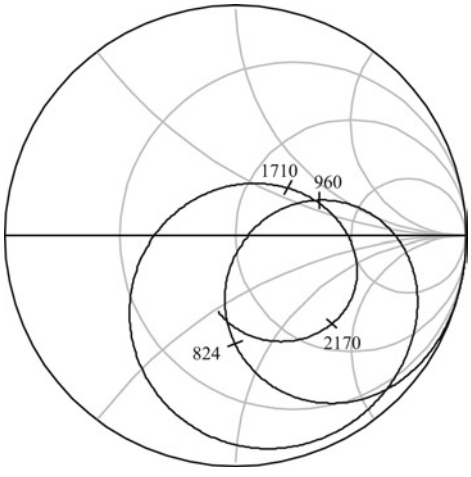

Fig. 3 *Simulated input impedance of radiating element without balun/matching network, Z_{rad}*

large bandwidth in terms of impedance, as can be seen in Fig. 2, it is far from sufficient to cover the complete 824–960 and 1710–2170 MHz frequency bands.

2.2 Balun

The balun is based on a Marchand balun [12] of third-order (i.e. three stubs), which essentially is a microstrip to co-planar stripline (CPS) transition with associated $\lambda/4$-stubs [18]. In a dual-band application in which the frequency bands are separated by a factor of 2, the standard $\lambda/4$ short-circuited CPS stub at the microstrip to CPS transition cannot be used because it would short-circuit the upper band signals at the transition (the stub at 1800 MHz is $\simeq\lambda/2$ long and would therefore transform the short circuit into another short circuit instead of the desired open). This stub was therefore replaced with a true open circuit. When utilising the balun as an impedance-transforming network, there are six degrees of freedom available corresponding to the electrical lengths βl, where l is the physical length of the stub and $\beta = 2\pi/\lambda_g$ is the guided wavenumber of the transmission line structure, and corresponding characteristic impedances (Z_0, in Ω) of each of the three stubs (two microstrips and one CPS). In this paper, the antenna was manufactured on 0.8 mm FR-4 substrate ($\varepsilon_r = 4.44$), limiting the possible characteristic impedances of microstrip lines to $\simeq$60–100 and 85–135 Ω for the CPS line. For the microstrip lines, the lower limit is set by size constraints; the ground for the microstrip is one of the CPS lines, which should be at least three times the width of the microstrip resulting in very large CPS lines for low-impedance microstrips. The upper limit is determined by manufacturing tolerances and what losses are acceptable; in this case, 100 Ω corresponds to $\simeq$0.5 mm strips. Higher impedances can, in principle, be obtained by using a thicker dielectric, but in this application, the thickness was limited by excessive radiation of the open-ended series microstrip stub at the upper frequency band. Simulated circuit Q-values of less than 4 was obtained for the series stub when implemented on a 1.5 mm thick substrate. For the CPS line, the lower limit is mainly set by manufacturing tolerances and the metal thickness; in this case, 85 Ω corresponds to a 0.2 mm gap and 35 μm thick copper metal. The upper limit is again set by size constraints.

2.3 Impedance matching

The simulated input impedance Z_{rad} of the radiating element, without balun, is shown in Fig. 3. The long dipole is designed for a resonant frequency approximately at the centre of the lower band. The short dipole is operating above its resonant frequency to give a more suitable impedance locus for the impedance transformations introduced by the balun. The effect of the parasitic shunt capacitance between the feed terminals is clearly seen at the upper frequency band of 1710–2170 MHz, shifting the impedance loci to the capacitive and high-impedance region of the Smith chart. The radiating element is connected to a CPS line. The CPS line, with characteristic impedance $Z_{CPS} = 92\ \Omega$ and electrical length $(\beta l)_{CPS} = 84^\circ$ at 900 MHz (Table 1), rotates the impedances of the antenna element seen in Fig. 3 into the values in Fig. 4 according to (1).

$$Z_{rad+CPS} = Z_{CPS}\frac{Z_{rad} + jZ_{CPS}\tan\beta l}{Z_{CPS} + jZ_{rad}\tan\beta l} \quad (1)$$

The upper frequency band is shifted only little because of the $\simeq\lambda/2$ length of the line at 1800 MHz, the main effect instead being an extension of the curve. The lower band however has been shifted a half turn into the inductive region.

The open microstrip series stub, with $Z_{MS1} = 60\ \Omega$ and $(\beta l)_{MS1} = 55^\circ$ at 900 MHz (referenced to the centre of the CPS line), adds the impedance $Z_{in,MS1} = -jZ_{MS1}\cot(\beta l)_{MS1}$ to $Z_{rad+CPS}$. At the lower frequency band, $Z_{in,MS1}$ introduces a series reactance of $-j42\ \Omega$ (at 900 MHz), thus moving the entire band closer to 50 Ω. At the upper frequency band, the stub looks like a series inductance with negligible reactance at 1700 MHz but $+j59\ \Omega$ at 2.2 GHz, improving the match at the upper limit of the upper frequency band. The final microstrip line, with $Z_{MS2} = 70\ \Omega$ and $(\beta l)_{MS2} = 38^\circ$ at 900 MHz, rotates both curves closer to 50 Ω, giving the impedances shown in Fig. 5. The complete circuit model for the balun/matching network is shown in Fig. 6.

No losses were included in the simulations of the matching network to make sure that the bandwidth enhancement stems from the compensation of reactances and not by extra losses introduced by the transmission lines.

Table 1: Transmission line properties at 900 MHz

	Z_0 (Ω)	ε_r	λ_g (mm)	l (mm)	βl (degree)
MS line	70	3.4	181.5	19.2	38°
MS stub	60	3.5	178.9	27.3	55°
CPS line	92	2.0	233.8	54.4	84°

3 Measurement results

The antenna was manufactured on 0.8 mm FR-4 (approximately $\varepsilon_r = 4.44$ and $\tan\delta = 0.02$) substrate, in which a minimum slot width of 0.2 mm was mandated by the used technology. Impedance measurements were obtained using an Agilent PNA E8364B network analyser and are presented together with simulated results in Fig. 7, this time with losses included in the simulated data. Simulated and measured results are in excellent agreement, apart from the upper frequency band being broader than expected. Although such deviations are typically attributed to the high dielectric losses of the FR-4 substrate, the high return loss at 3 GHz gives an indication that that might not be the case here, which was also confirmed in the efficiency measurement described subsequently.

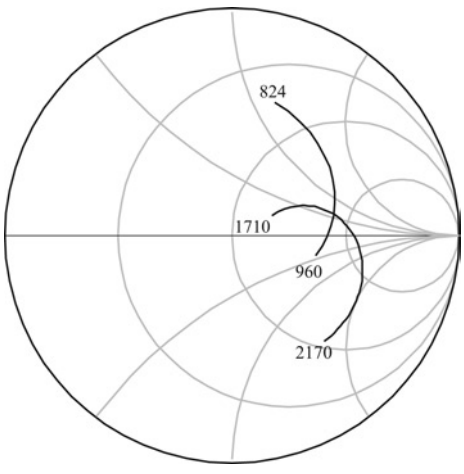

Fig. 4 *Simulated input impedance of radiating element and CPS line, $Z_{rad+CPS}$*

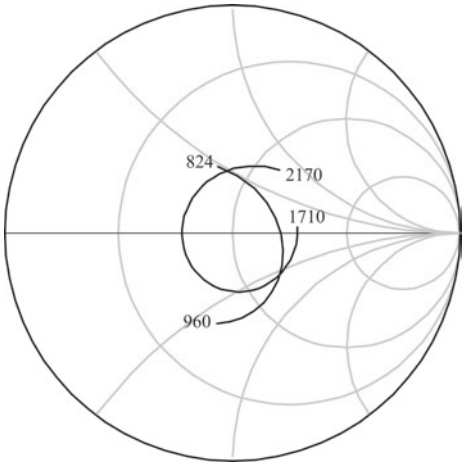

Fig. 5 *Simulated input impedance of complete antenna, Z_{in}*

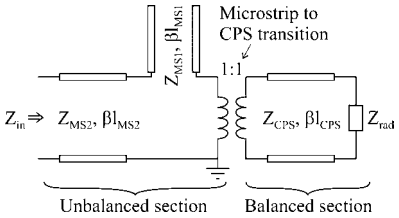

Fig. 6 *Equivalent circuit model of balun/matching network*

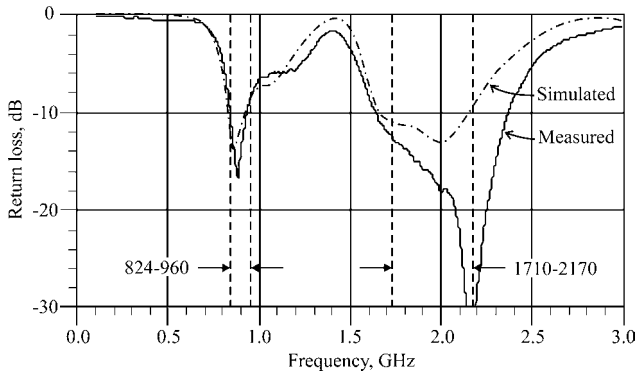

Fig. 7 *Measured and simulated return loss of complete antenna*

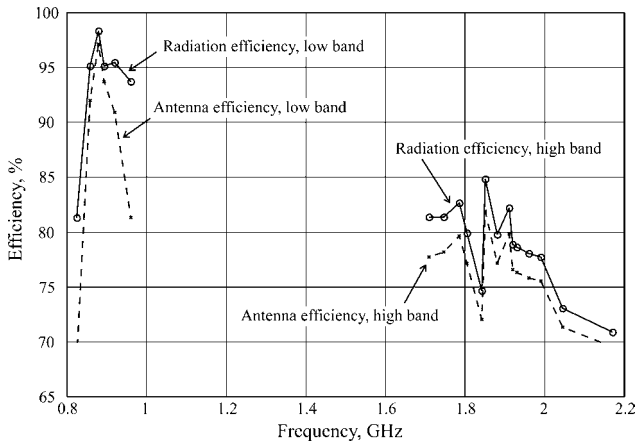

Fig. 8 *Measured efficiency of complete antenna*

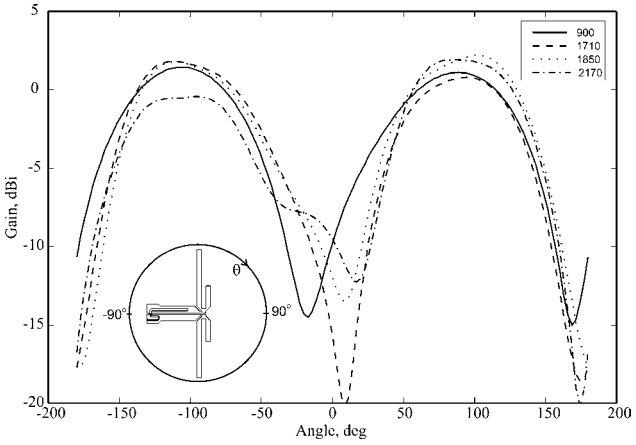

Fig. 9 *Measured E-plane radiation gain, $\varphi = 0^\circ$*

The radiation properties and antenna efficiency, as defined by $\eta_{ant} = \eta_{rad} \times (1 - |\Gamma|^2)$, where Γ is the reflection coefficient at the input port, were measured using a Satimo STARGATE-64 near-field chamber [19]. η_{ant} is shown in Fig. 8 together with the radiation efficiency as defined by $\eta_{rad} = P_{rad}/(P_{rad} + P_{loss})$. The difference between η_{ant} and η_{rad} represents the effect of the impedance mismatch, and as can be seen in Fig. 8, there is not much additional improvement that can be achieved through matching. The reduction of efficiency at the upper frequency band could be improved by using a more expensive microwave substrate rather than standard low-cost FR-4.

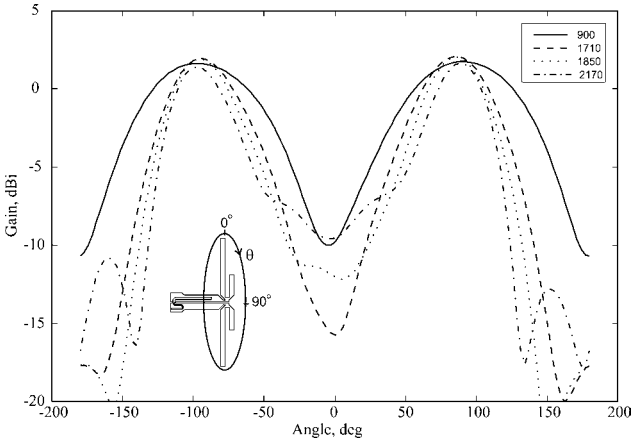

Fig. 10 *Measured E-plane radiation gain, $\varphi = 90^\circ$*

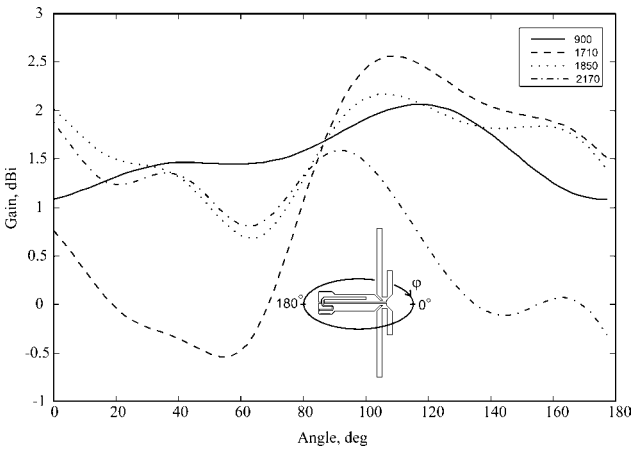

Fig. 11 *Measured H-plane radiation gain, $\theta = 90^\circ$*

The measured realised gain (i.e. including mismatch loss) is shown in Figs. 9–11, with one frequency in the low band (900 MHz) and three frequencies in the high band (1710, 1850, 2170 – end and middle frequencies of the supported bands). Not much gain variation over the frequency range can be observed. Figs. 9 and 10 show the expected higher gain of the upper frequency band, probably caused by the low-frequency-radiating element acting as a reflector. This also affects the H-plane radiation (Fig. 11), in which there is an increased gain variation compared with the lower frequencies. The asymmetry in the feeding network might also have some influence on the gain variation. For symmetry reasons, only the angles between 0° and 180° have been plotted in Fig. 11.

4 Conclusions

A dual wideband dipole antenna concept has been presented. By using a Marchand balun modified for dual frequency operation and co-optimised with the radiating element, two resonances are obtained in each band, giving a wide impedance bandwidth. The concept has been demonstrated with an implementation on FR-4 substrate, covering the popular wireless bands GSM850/900/1800/1900 + WCDMA 2.1 GHz. Detailed descriptions of the radiating element and the effect of the matching components have been provided. Despite using low-cost substrate, high antenna efficiency has been obtained. The measured radiation patterns in all principal planes show only a minor dependency on frequency.

5 References

1 Stoiljkovic, V., Suganthan, S., and Benhaddou, M.: 'A novel dual-band centre-fed printed dipole antenna'. IEEE Antennas and Propagation Society Int. Symp., 2003, vol. 2, pp. 938–941

2 Chen, H.-M., Chen, J.-M., Cheng, P.-S., and Lin, Y.-F.: 'Feed for dual-band printed dipole antenna', *IEE Electron. Lett.*, 2004, **40**, pp. 1320–1322

3 Boifot, A.M.: 'Shortened, directive dipole for array antennas', Int. J. Electron., 1991, **71**, (1), pp. 127–137

4 Jeon, S., Yu, Y., Kahng, S., Park, J., Kim, N., and Choi, J.: 'Dual-band dipole antenna for ISO 18000–6/ISO 18000–4 passive RFID tag applications'. IEEE Antennas and Propagation Society Int. Symp., 2006, pp. 4285–4288

5 Suh, S.-Y., Waltho, A.E., Krishnamurthy, L., Souza, D., Gupta, S., Pan, H.K., and Nair, V.K.: 'A miniaturized dual-band dipole antenna with a modified meander line for laptop computer application in the 2.5 and 5.25 GHz WLAN band'. IEEE Antennas and Propagation Society Int. Symp., 2006, pp. 2617–2620

6 Su, C.-M., Chen, H.-T., and Wong, K.-L.: 'Printed dual-band dipole antenna with U-slotted arms for 2.4/5.2 GHz WLAN operation', *Electron. Lett.*, 2002, **38**, pp. 1308–1309

7 Zhang, Z., Iskander, M.F., Langer, J.-C., and Mathews, J.: 'Wideband dipole for WLAN'. IEEE Antennas and Propagation Society Int. Symp, 2004, vol. 2, pp. 1963–1966

8 Zhang, Z., Iskander, M.F., Langer, J.-C., and Mathews, J.: 'Dual-band WLAN dipole antenna using an internal matching circuit', *IEEE Trans. Antennas Propag.*, 2005, **53**, pp. 1813–1818

9 Tefiku, F., and Grimes, C.A.: 'Design of broad-band and dual-band antennas comprised of series-fed printed-strip dipole pairs', *IEEE Trans. Antennas Propag.*, 2000, **48**, pp. 895–900

10 Kim, M.J., Cho, C.S., and Kim, J.: 'A dual band printed dipole antenna with spiral structure for WLAN application', *IEEE Microw. Wirel. Compon. Lett.*, 2005, **15**, pp. 910–912

11 Suh, Y.-H., and Chang, K.: 'Low cost microstrip-fed dual frequency printed dipole antenna for wireless communications', *Electron. Lett.*, 2000, **36**, pp. 1177–1179

12 Trifunovic, V., and Jokanovic, B.: 'Review of printed Marchand and double Y baluns: characteristics and application', *IEEE Trans. Microw. Theory Tech.*, 1994, **42**, pp. 1454–1462

13 Edwards, B., and Rees, D.: 'A broadband printed dipole with integrated balun', *Microw. J.*, May 1987, pp. 339–344

14 Michishita, N., Arai, H., Nakano, M., Satoh, T., and Matsuoka, T.: 'FDTD analysis for printed dipole antenna with balun'. Asia-Pacific Microwave Conf., 2000, pp. 739–742

15 Scott, M.: 'A printed dipole for wide-scanning array application'. 11th Int. Conf. on Antennas and Propagation, 2001, vol. 1, pp. 37–40

16 Delaveaud, C., and Brocheton, C.: 'Dual-band behaviour of printed dipole', *Electron. Lett.*, 2000, **36**, pp. 1175–1177

17 IE3D v.10, (Zeland Software, Fremont, CA)

18 Axelrod, A., and Lipman, D.: 'Novel planar balun feeds octave-bandwidth dipole', Microwaves & RF, August 1986, pp. 91–92

19 Iversen, P.O., Garreau, P., and Burrel, D.: 'Real-time spherical near-field handset antenna measurements', *IEEE Antennas Propag. Mag.*, 2001, **43**, (3), pp. 90–94